Computer Assisted Mechanics and Engineering Sciences, 11: 265–274, 2004.

Application of meshless element free Galerkin method in two-dimensional heat conduction problems

I. V. Singh, K. Sandeep and R. Prakash
Mechanical Engineering Group, Birla Institute of Technology and Science, Pilani, 333031, Rajasthan, India

(Received September 11, 2002)

In this paper, meshless element free Galerkin method has been used to obtain the numerical solution of transient and steady state heat conduction problems in two-dimensional domains. The unknown function of temperature $T(\mathbf{x})$ has been approximated by moving least square approximant $T^h(\mathbf{x})$. These approximants are constructed by using a weight function, a polynomial basis and a set of non-constant coefficients. Variational method is used to obtain the discrete equations. Essential boundary conditions are imposed by Lagrange multiplier technique. Two new weight functions namely hyperbolic and rational have been proposed. The results have been obtained for a two-dimensional model problem using different EFG weight functions and are compared with those obtained by finite element and analytical methods.

Keywords: meshless method, element free Galerkin method, two-dimensional transient and steady heat conduction

NOTATIONS

a – elemental (cell) area,
$a_j(x,y)$ – non constant coefficients,
c – specific heat of the material,
d_{mxI}, d_{myI} – size of the domain of influence at I^{th} node in x and y directions,
$d_{\max}$ – scaling parameter,
h – convective heat transfer coefficient,
k – coefficient of thermal conductivity,
$p_j(x,y)$ – polynomial basis function,
$\dot{Q}$ – rate of internal heat generation per unit volume,
$T^h(x,y)$ – moving least square approximant,
T_e – edge temperature,
T_∞ – surrounding temperature,
T_{ini} – initial temperature,
t – time,
$T_{,x}, T_{,y}$ – $\dfrac{\partial T}{\partial x}, \dfrac{\partial T}{\partial y}$,
$T_{,xx}, T_{,yy}$ – $\dfrac{\partial^2 T}{\partial x^2}, \dfrac{\partial^2 T}{\partial y^2}$,
$\dot{T}$ – $\dfrac{\partial T}{\partial t}$,
$w(\mathbf{x}-\mathbf{x}_I)$ – weight function,
δ – variational parameter,

λ – Lagrangian multiplier,
Ω – two-dimensional domain,
$\Phi(\mathbf{x})$ – shape function,
Γ – boundary of the domain,
ρ – mass density.

1. Introduction

Different numerical techniques have been used to solve transient and steady state heat conduction problems. The point-matching technique was used by Sparrow [5] to obtain the temperature distribution inside an irregular shape system. France [4] obtained analytical series solution for steady-state heat conduction problems with irregular shaped boundaries. The probability method was used by Sheikh and Sparrow [1] to solve steady state and transient heat conduction problems of arbitrary shapes with arbitrary boundary conditions. Khader and Hanna [16] used an iterarative boundary integral numerical solution for steady state heat conduction problems. Monte Carlo method was used by Fraley [21] to solve transient heat conduction problems. Beck [10] used Green's function solution technique to solve transient heat conduction problems for different set of boundary conditions. Lapace transform technique is being used by Ozisik [17] to solve transient heat transfer problems. At present, most of the transient heat conduction problems are solved by finite difference method [11], graphical method [6] and finite element method [20].

In all these methods, finite element technique can be considered as the most general technique for steady state and transient heat conduction problems. The finite element method (FEM) has been successfully applied in solving variety of problems in heat transfer. In this method, the function over the solution domain is approximated by a polynomial over a small domain, known as finite element. The discretization of domain into small elements is very time-consuming process. Therefore, there is a need of a method that may be somewhat more expansive from the viewpoint of the computer time but requires less time in the preparation of the data.

In recent years, few new techniques have been developed, named as meshless methods. First meshless method is developed by Lucy [15], which is known as smooth particle hydrodynamic (SPH) method [12, 14]. Moving least square (MLS) approximants are first used by Nayroles [2] to develop Galerkin equations, called diffuse element method (DEM). This method has been refined by Belytschko et al., known as element free Galerkin (EFG) method [24, 29]. The other meshless method include partition of unity method (PUM) [9, 13], hp-cloud method [3], reproducing kernel particle method (RKPM) [28], method of finite spheres [23], free mesh method (FMM) [7], local boundary integral equation (LBIE) method [27], meshless local Petrov–Galerkin (MLPG) method [22], natural element method (NEM) [18] and natural neighbour Galerkin method [19].

In this paper, EFG method has been used to discretize the space domain of steady state and transient heat conduction problems. In EFG method, function approximation is done entirely in terms of nodes and integration over solution domain needs only integration cell to obtain the solution. Although this method is more expansive from the viewpoint of computational time but requires less time in the preparation of data. Crank–Nicolson technique has been used for discretization of time domain. Two dimensional steady state and transient heat conduction model problems have been solved by using different weight functions. The results obtained by EFG method, are compared with those obtained by finite element and analytical methods [8].

2. The EFG method

The discretization of the governing equations by element free Galerkin method requires moving least square (MLS) interpolation functions which are made up of three components: a weight function

associated with each node, a polynomial basis and a set of non constant coefficients. The weight function is non-zero over a small neighborhood at a particular node, called support of the node.

Moving least square approximation

Using moving least square approximation, the unknown function $T(x, y)$ is approximated by $T^h(x,\ y)$ over the domain Ω [24]

$$T^h(x,y) = \sum_{j=1}^{m} p_j(x,y)\, a_j(x,y) \equiv \mathbf{p}^{\mathrm{T}}(x,y)\, \mathbf{a}(x,y) \equiv \mathbf{p}^{\mathrm{T}}(\mathbf{x})\, \mathbf{a}(\mathbf{x}) \tag{1}$$

where m is number of terms in the basis, $p_j(x\,,\, y)$ is monomial basis function, $a_j(x\,,\, y)$ is non-constant coefficients,

$$\mathbf{x}^{\mathrm{T}} = [x \quad y], \qquad \mathbf{p}^{\mathrm{T}}(\mathbf{x}) = [1 \quad x \quad y].$$

The coefficients $a_j(\mathbf{x})$ are found by minimizing the quadratic functional $J(\mathbf{x})$ given by

$$J(\mathbf{x}) = \sum_{I=1}^{n} w(\mathbf{x}-\mathbf{x}_I) \left\{ \sum_{j=1}^{m} p_j(\mathbf{x}_I)\, a_j(\mathbf{x}) - T_{\mathbf{I}} \right\}^2 \tag{2}$$

where $w(\mathbf{x}-\mathbf{x}_I)$ is a weight function which is non zero over a small domain, called domain of influence. n is the number of nodes in the domain of influence.

The minimization of $J(\mathbf{x})$ w.r.to $\mathbf{a}(\mathbf{x})$ leads the following set of equations

$$\mathbf{a}(\mathbf{x}) = \mathbf{A}^{-1}(\mathbf{x})\, \mathbf{B}(\mathbf{x})\, \mathbf{T}, \tag{3}$$

where $\mathbf{A}$ and $\mathbf{B}$ are given as

$$\mathbf{A} = \sum_{I=1}^{n} w(\mathbf{x}-\mathbf{x}_I)\, \mathbf{p}(\mathbf{x}_I)\, \mathbf{p}^{\mathrm{T}}(\mathbf{x}_I)$$

$$= w(\mathbf{x}-\mathbf{x}_1) \begin{bmatrix} 1 & x_1 & y_1 \\ x_1 & x_1^2 & x_1 y_1 \\ y_1 & x_1 y_1 & y_1^2 \end{bmatrix} + w(\mathbf{x}-\mathbf{x}_2) \begin{bmatrix} 1 & x_2 & y_2 \\ x_2 & x_2^2 & x_2 y_2 \\ y_2 & x_2 y_2 & y_2^2 \end{bmatrix}$$

$$+ \ldots w(\mathbf{x}-\mathbf{x}_n) \begin{bmatrix} 1 & x_n & y_n \\ x_n & x_n^2 & x_n y_n \\ y_n & x_n y_n & y_n^2 \end{bmatrix}, \tag{4}$$

$$\mathbf{B}(\mathbf{x}) = [w(\mathbf{x}-\mathbf{x}_1)\, \mathbf{p}(\mathbf{x}_1), w(\mathbf{x}-\mathbf{x}_2)\, \mathbf{p}(\mathbf{x}_2), \ldots\ldots\ldots\ldots\ldots\ldots w(\mathbf{x}-\mathbf{x}_n)\, \mathbf{p}(\mathbf{x}_n)]$$

$$= \left[w(\mathbf{x}-\mathbf{x}_1) \begin{bmatrix} 1 \\ x_1 \\ y_1 \end{bmatrix}, w(\mathbf{x}-\mathbf{x}_2) \begin{bmatrix} 1 \\ x_2 \\ y_2 \end{bmatrix}, \ldots\ldots\ldots\ldots\ldots w(\mathbf{x}-\mathbf{x}_n) \begin{bmatrix} 1 \\ x_n \\ y_n \end{bmatrix} \right], \tag{5}$$

$$\mathbf{T}^{\mathrm{T}} = [T_1, T_2, \ldots T_n]. \tag{6}$$

By substituting Eq. (3) in Eq. (1), the MLS approximants can be defined as

$$T^h(\mathbf{x}) = \sum_{I=1}^{n} \Phi_I(\mathbf{x}) T_I = \mathbf{\Phi}(\mathbf{x})\mathbf{T} \tag{7}$$

where the shape function $\Phi_I(\mathbf{x})$ is defined by

$$\Phi_I(\mathbf{x}) = \sum_{j=0}^{m} p_j(\mathbf{x})(\mathbf{A}^{-1}(\mathbf{x})\mathbf{B}(\mathbf{x}))_{jI} = \mathbf{p}^{\mathrm{T}}\mathbf{A}^{-1}\mathbf{B}_I. \tag{8}$$

The derivative of the shape function is given as

$$\Phi_{I,\mathbf{x}}(\mathbf{x}) = (\mathbf{p}^{\mathrm{T}}\mathbf{A}^{-1}\mathbf{B}_I)_{,\mathbf{x}} = \mathbf{p}^{\mathrm{T}}_{,\mathbf{x}}\mathbf{A}^{-1}\mathbf{B}_I + \mathbf{p}^{\mathrm{T}}(\mathbf{A}^{-1})_{,\mathbf{x}}\mathbf{B}_I + \mathbf{p}^{\mathrm{T}}\mathbf{A}^{-1}(\mathbf{B}_I)_{,\mathbf{x}}. \tag{9}$$

Weight function description

The weight function is non-zero over a small neighborhood of $\mathbf{x}_I$, called the domain of influence of node I. The shape of this domain is arbitrary but in the present analysis rectangular domain is preferred [24]. The choice of weight function $w(\mathbf{x} - \mathbf{x}_I)$ affects the resulting approximation $T^h(\mathbf{x}_I)$. In this paper, two new weight function namely hyperbolic and rational weight functions have been proposed. The different weight functions used in the present analysis can be written as a function of normalized radius r as follows:

The gaussian weight function [25]

$$w(\mathbf{x} - \mathbf{x}_I) = w(r) = \left\{ \begin{array}{cc} e^{-(2.5r)^2} & 0 \le r \le 1 \\ 0 & r > 1 \end{array} \right\}. \tag{10a}$$

The quartic-spline weight function [26]

$$w(\mathbf{x} - \mathbf{x}_I) = w(r) = \left\{ \begin{array}{cc} 1 - 6r^2 + 8r^3 - 3r^4, & 0 \le r \le 1 \\ 0 & r > 1 \end{array} \right\}. \tag{10b}$$

The hyperbolic weight function

$$w(\mathbf{x} - \mathbf{x}_I) = w(r) = \left\{ \begin{array}{cc} \mathrm{sech}\,(r+3) & 0 \le r \le 1 \\ 0 & r > 1 \end{array} \right\}. \tag{10c}$$

The rational weight function

$$w(\mathbf{x} - \mathbf{x}_I) = w(r) = \left\{ \begin{array}{cc} \dfrac{1}{r^2 + 0.1} & 0 \le r \le 1 \\ 0 & r > 1 \end{array} \right\}, \tag{10d}$$

where

$$(r_x)_I = \frac{\| x - x_I \|}{d_{mxI}} \quad \text{and} \quad (r_y)_I = \frac{\| y - y_I \|}{d_{myI}},$$

$$d_{mxI} = d_{\max} \,.c_{xI} \quad \text{and} \quad d_{myI} = d_{\max} \,.c_{yI},$$

$d_{\max}$ – scaling parameter.

c_{xI} and c_{yI} at node I, are the distances to the nearest neighbors. d_{mxI} and d_{myI} are chosen such that the matrix is non-singular everywhere in the domain.

The weight function at any given point can be calculated as

$$w(\mathbf{x} - \mathbf{x}_I) = w(r_x).w(r_y) = w_x.w_y \tag{11a}$$

where $w(r_x)$ or $w(r_y)$ can be calculated by replacing r by r_x or r_y in the expression of $w(r)$.

The derivatives of the weight function are obtained as

$$w_{,x} = \frac{\mathrm{d}w_x}{\mathrm{d}x}.w_y, \qquad w_{,y} = \frac{\mathrm{d}w_y}{\mathrm{d}y}.w_x. \tag{11b}$$

3. Discretization and numerical implementation

A two-dimensional transient heat conduction equation for isotropic material is

$$k\,(T_{,xx}+T_{,yy})+\dot{Q}-\rho c\dot{T}=0. \tag{12a}$$

The Initial conditions are

$$\text{at } t=0, \qquad T=T_{\text{ini}} \qquad \text{in } \Omega. \tag{12b}$$

The boundary conditions are

$$\begin{aligned} &\text{at edge } \Gamma_1, && T=T_e,\\ &\text{at edge } \Gamma_2, && kT_{,y}=0,\\ &\text{at edge } \Gamma_3, && -kT_{,x}=h(T-T_\infty),\\ &\text{at edge } \Gamma_4, && -kT_{,y}=h(T-T_\infty). \end{aligned} \tag{12c}$$

The weak form of the Eq. (12a) with the boundary conditions is obtained as

$$\begin{aligned} &-\int_\Omega [k\,(w_{,x}T_{,x}+w_{,y}T_{,y})]\,\mathrm{d}\Omega+\int_\Omega w\,\dot{Q}\,\mathrm{d}\Omega-\int_\Omega \rho c w\dot{T}\,\mathrm{d}\Omega\\ &\quad-\int_{\Gamma_3} w h\,(T-T_\infty)\,\mathrm{d}\Gamma_3-\int_{\Gamma_4} w h\,(T-T_\infty)\,\mathrm{d}\Gamma_4=0. \end{aligned} \tag{13}$$

The functional $\Pi(T)$ can be written as

$$\begin{aligned} \Pi(T)=&\int_\Omega \frac{k}{2}\left[T_{,x}^2+T_{,y}^2\right]\mathrm{d}\Omega+\int_\Omega \rho\,c\,T\,\dot{T}\,\mathrm{d}\Omega-\int_\Omega T\,\dot{Q}\,\mathrm{d}\Omega+\int_{\Gamma_3}\frac{hT^2}{2}\mathrm{d}\Gamma_3\\ &+\int_{\Gamma_4}\frac{hT^2}{2}\mathrm{d}\Gamma_4-\int_{\Gamma_3} hT T_\infty\,\mathrm{d}\Gamma_3-\int_{\Gamma_4} hT T_\infty\,\mathrm{d}\Gamma_4. \end{aligned} \tag{14}$$

Enforcing essential boundary conditions using Lagrange multipliers, the functional $\Pi^*(T)$ is obtained as

$$\begin{aligned} \Pi^*(T)=&\int_\Omega \frac{k}{2}\left[T_{,x}^2+T_{,y}^2\right]\mathrm{d}\Omega+\int_\Omega \rho\,c\,T\,\dot{T}\,\mathrm{d}\Omega-\int_\Omega T\,\dot{Q}\,\mathrm{d}\Omega+\int_{\Gamma_3}\frac{hT^2}{2}\mathrm{d}\Gamma_3+\int_{\Gamma_4}\frac{hT^2}{2}\mathrm{d}\Gamma_4\\ &-\int_{\Gamma_3} hT T_\infty\,\mathrm{d}\Gamma_3-\int_{\Gamma_4} hT T_\infty\,\mathrm{d}\Gamma_4+\int_{\Gamma_1}\lambda\,(T-T_e)\,\mathrm{d}\Gamma_1. \end{aligned} \tag{15}$$

Using Variational principle, Eq. (15) reduces to

$$\begin{aligned} \delta\Pi^*(T)=&\int_\Omega k\left[T_{,x}^{\mathrm{T}}\delta T_{,x}+T_{,y}^{\mathrm{T}}\delta T_{,y}\right]\mathrm{d}\Omega+\int_\Omega \rho\,c\,\dot{T}\,\delta T\,\mathrm{d}\Omega-\int_\Omega \dot{Q}\,\delta T.\mathrm{d}\Omega+\int_{\Gamma_3} h\,T\,\delta T\,\mathrm{d}\Gamma_3\\ &+\int_{\Gamma_4} hT\,\delta T\,\mathrm{d}\Gamma_4-\int_{\Gamma_3} hT_\infty\delta T\,\mathrm{d}\Gamma_3-\int_{\Gamma_4} hT_\infty\delta T\,\mathrm{d}\Gamma_4\\ &+\int_{\Gamma_1}\lambda\,\delta T\,\mathrm{d}\Gamma_1+\int_{\Gamma_1}\delta\lambda\,(T-T_e)\,\mathrm{d}\Gamma_1. \end{aligned} \tag{16}$$

Since δT and $\delta\lambda$ are arbitrary in preceding equation, the following relations are obtained by using Eq. (7)

$$[\mathbf{K}]\{\mathbf{T}\}+[\mathbf{C}]\{\dot{\mathbf{T}}\}+[\mathbf{G}]\{\boldsymbol{\lambda}\}=\{\mathbf{f}\}, \tag{17a}$$

$$[\mathbf{G}^{\mathrm{T}}]\{\mathbf{T}\} = \{\mathbf{q}\}, \tag{17b}$$

where

$$K_{IJ} = \int_{\Omega} \begin{bmatrix} \boldsymbol{\Phi}_{I,x} \\ \boldsymbol{\Phi}_{I,y} \end{bmatrix} \begin{bmatrix} k & 0 \\ 0 & k \end{bmatrix} \begin{bmatrix} \boldsymbol{\Phi}_{J,x} \\ \boldsymbol{\Phi}_{J,y} \end{bmatrix} \mathrm{d}\Omega + \int_{\Gamma_3} h\boldsymbol{\Phi}_I^{\mathrm{T}}\boldsymbol{\Phi}_J \mathrm{d}\Gamma_3 + \int_{\Gamma_4} h\boldsymbol{\Phi}_I^{\mathrm{T}}\boldsymbol{\Phi}_J \mathrm{d}\Gamma_4, \tag{18a}$$

$$C_{IJ} = \int_{\Omega} \boldsymbol{\Phi}_I^{\mathrm{T}} \begin{bmatrix} \rho c & 0 \\ 0 & \rho c \end{bmatrix} \boldsymbol{\Phi}_J \, \mathrm{d}\Omega, \tag{18b}$$

$$G_{IK} = \int_{\Gamma_1} \boldsymbol{\Phi}_I N_K \mathrm{d}\Gamma_1, \tag{18c}$$

$$f_I = \int \dot{Q}\boldsymbol{\Phi}_I \mathrm{d}\Omega + \int_{\lambda_3} h.T_{\infty}\boldsymbol{\Phi}_I.\mathrm{d}\lambda_3 + \int_{\lambda_4} h.T_{\infty}\boldsymbol{\Phi}_I.\mathrm{d}\lambda_4, \tag{18d}$$

$$q_K = \int_{\Gamma_1} T_e N_K \mathrm{d}\Gamma_1. \tag{18e}$$

Using Crank–Nicolson method for time approximation, the Eq. (17) can be written as

$$\left[\begin{array}{c:c} \mathbf{K}^* + \mathbf{C} & \mathbf{G} \\ \hdashline \mathbf{G}^{\mathrm{T}} & 0 \end{array}\right] \left\{ \begin{array}{c} \mathbf{T}_n \\ \boldsymbol{\lambda} \end{array} \right\} = \left\{ \begin{array}{c} \mathbf{R}_n \\ \mathbf{q} \end{array} \right\} \tag{19}$$

where

$$\mathbf{R}_n = ([\mathbf{C}] - (1-\alpha)\Delta t\,[\mathbf{K}])\{\mathbf{T}\}_{n-1} + \alpha\Delta t\,\{\mathbf{f}\}_n + (1-\alpha)\Delta t\{\mathbf{f}\}_{n-1}, \tag{20a}$$

$$\mathbf{K}^* = \alpha\Delta t[\mathbf{K}]. \tag{20b}$$

4. Numerical results and discussion

The parameters considered for the transient analysis of the model shown in Fig. 1 are tabulated in Table 1. Table 2 shows, a comparison of results obtained by EFG method for different weight functions with the results of finite element method at the corner ($x = L$, $y = W/2$) for 121 nodes. A similar comparison of results has also been shown in Fig. 2 at the center ($x = L/2$, $y = 0$) of the model for the same number of nodes.

The parameters considered for the steady state analysis of the model shown in Fig. 1 are tabulated in Table 3. The EFG results for the steady state analysis of the model by using different weight functions have been compared in Table 4 with analytical and finite element results. The L_2-error has also been calculated for different weight functions EFG and FEM with analytical solution and is given in Table 5. The L_2-error has been plotted in Fig. 3 for the calculation of rate of convergence. The rate of convergence for quarticspline, gaussian, hyperbolic, rational and FEM are obtained as 0.5153, 0.4821, 0.8232, 0.5170 and 0.4752. It can be noted from these results that the hyperbolic weight function has the greatest rate of convergence and FEM has least rate of convergence.

It can be noted from the tables and figures that the EFG results are converged and in good agreement with the results of finite element and analytical methods. From the analysis, it is clear that the EFG method is very much efficient for two-dimensional steady state and transient heat conduction problems. For high accuracy, large number of nodes can be easily generated with least effort. This work can be extended for the thermal analysis of three-dimensional composite structures using EFG method.

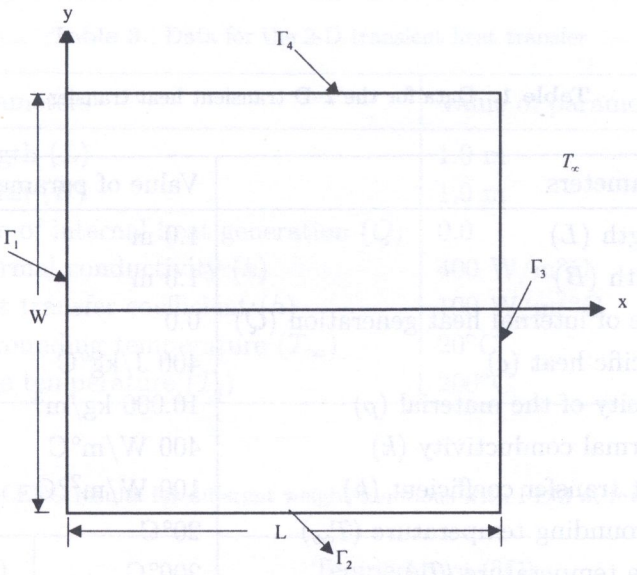

Fig. 1. Two-dimensional model for transient and steady state heat transfer

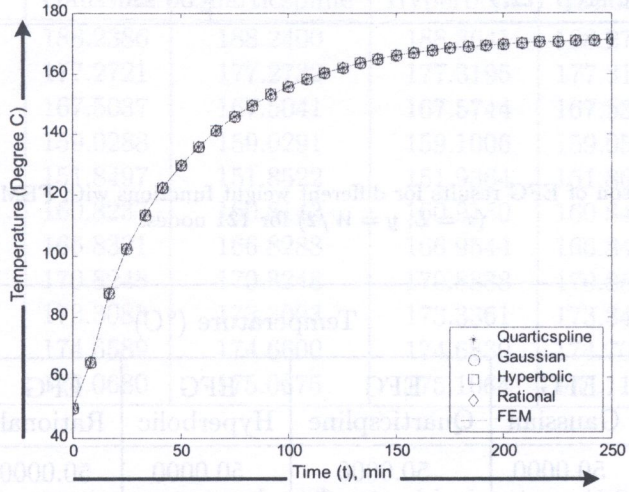

Fig. 2. Comparison EFG results for different weight functions with FEM at the center point $(x = L/2,\ y = 0)$

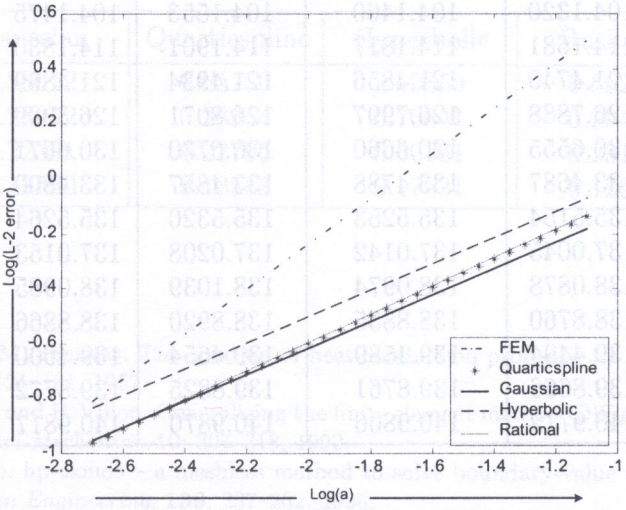

Fig. 3. A plot of L_2 – errorfor different weight of EFG and FEM

Table 1. Data for the 2–D transient heat transfer

Parameters	Value of parameters
Length (L)	1.0 m
Width (B)	1.0 m
Rate of internal heat generation ($\dot{Q}$)	0.0
Specific heat (c)	400 J/kg°C
Density of the material (ρ)	10.000 kg/m^3
Thermal conductivity (k)	400 W/m°C
Heat transfer coefficient (h)	100 W/m^2°C
Surrounding temperature (T_∞)	20°C
Edge temperature (T_e)	200°C
Initial temperature (T_{ini})	50°C
Time step (Δt)	50 sec

Table 2. Comparison of EFG results for different weight functions with FEM at the corner point ($x = L$, $y = W/2$) for 121 nodes.

Time (s) $t \times 10^3$	Temperature (°C)				
	EFG Gaussian	EFG Quarticspline	EFG Hyperbolic	EFG Rational	FEM
0	50.0000	50.0000	50.0000	50.0000	50.0000
1	51.1917	51.2044	51.2126	51.2057	51.5594
2	71.9143	71.9318	71.9433	71.9335	72.2840
3	90.3770	90.3929	90.4034	90.3945	90.6385
4	104.1320	104.1460	104.1553	104.1475	104.8925
5	114.1681	114.1817	114.1901	114.1830	114.7179
6	121.4740	121.4856	121.4934	121.4869	121.5636
7	126.7888	126.7997	126.8071	126.8009	126.8508
8	130.6555	130.6660	130.6730	130.6671	130.6977
9	133.4687	133.4788	133.4857	133.4800	133.4967
10	135.5154	135.5253	135.5320	135.5264	135.5332
11	137.0045	137.0142	137.0208	137.0153	136.0149
12	138.0878	138.0974	138.1039	138.0985	138.0929
13	138.8760	138.8855	138.8920	138.8866	138.8773
14	139.4494	139.4589	139.4654	139.4600	139.4479
15	139.8666	139.8761	139.8825	139.8772	139.8632
30	140.9712	140.9806	140.9870	140.9817	140.9628

Table 3. Data for the 2-D transient heat transfer

Parameters	Value of parameters
Length (L)	1.0 m
Width (B)	1.0 m
Rate of internal heat generation ($\dot{Q}$)	0.0
Thermal conductivity (k)	400 W/m°C
Heat transfer coefficient (h)	100 W/m^2°C
Surrounding temperature (T_∞)	20°C
Edge temperature (T_e)	200°C

Table 4. Comparison of EFG results for different weight functions with FEM at few locations for 121 nodes

Location (m)		Temperature (°C)				
X	Y	EFG Gaussian	EFG Quarticspline	EFG Hyperbolic	EFG Rational	FEM
0.2	0.0	188.2386	188.2400	188.3641	188.2767	188.2342
0.4	0.0	177.2721	177.2732	177.3195	177.3151	177.2753
0.6	0.0	167.5037	167.5041	167.5744	167.5381	167.5136
0.8	0.0	159.0288	159.0291	159.1006	159.0569	159.0416
1.0	0.0	151.8497	151.8522	151.9364	151.8626	151.8377
0.5	0.5	160.8237	160.8143	160.9150	160.8425	160.9319
0.5	0.3	166.8321	166.8288	166.9544	166.8428	166.8736
0.5	0.1	170.8248	170.8248	170.8838	170.8583	170.8398
0.5	− 0.1	173.3083	173.3093	173.3361	173.3491	173.3101
0.5	− 0.3	174.6589	174.6600	174.6830	174.7000	174.6559
0.5	− 0.5	175.0680	175.0675	175.1064	175.1169	175.0829

Table 5. L_2 – error in temperature for different weight functions of EFG and FEM

Elemental area/cell area (m^2)	EFG				FEM
	Gaussian	Quarticspline	Hyperbolic	Rational	
0.0625	0.58612	0.65150	2.49859	0.66269	0.59100
0.0156	0.28012	0.28954	0.70841	0.29473	0.76366
0.0100	0.22331	0.22796	0.60161	0.23181	0.23295
0.0025	0.12530	0.12543	0.17531	0.12686	0.13049

References

[1] A. Haji-Sheikh and E.M. Sparrow. The solution of heat conduction problems by probability methods. *Journal of Heat Transfer*, **89**: 121–131, 1967.

[2] B. Neyroles, G. Touzot and P. Villon. Generalizing the finite element method: Diffuse approximations and diffuse elements. *Computational Mechanics*, **10**: 307–318, 1992.

[3] C. Durate and J. Oden. hp-clouds – a meshless method to solve boundary-value problems. *Computer Methods in Applied Mechanics in Engineering*, **139**: 237–262, 1996.

[4] D.M. France. Analytical solution to steady state heat conduction problems with ir-regular shaped boundaries. *Journal of Heat Transfer*, **93**: 449–454, 1971.

[5] E.M. Sparrow. Temperature distribution & heat transfer results for internally cooled, heat generating solids, *Journal of Heat Transfer*, **82**: 389–392, 1960.
[6] F.P. Incropera and D.P. Dewitt. *Fundamentals of Heat and Mass Transfer*. John Wiley & Sons, Singapore 1990.
[7] G. Yagawa and T. Yamada. Free mesh method, a new meshless finite element method. *Compututational Mechanics*, **18**: 383–386, 1996.
[8] H.S. Carslaw and J.C. Jaeger. *Conduction of Heat in Solids*. Oxford University Press, London 1959.
[9] I. Babuska and J.M. Melenk. The partition of unity method. *International Journal for Numerical Methods in Engineering*, **40**: 727–758, 1997.
[10] J.V. Beck. Green's function solutions for transients heat conduction problems. *International Journal of Heat And Mass Transfer*, **27**: 1235–1244, 1984.
[11] J.P. Holman. *Heat Transfer*. Mc Graw-Hill, Inc., Singapore 1989.
[12] J.J. Monaghan. Smoothed particle hydrodynamics. *Annual Review of Astronomy & Astrophysics*, **30**: 543–574, 1992.
[13] J. Melenk and I. Babuska. The partition of unity method: Basic theory and applications. *Computer Methods in Applied Mechanics and Engineering*, **139**: 289–314, 1996.
[14] J. J. Monaghan. An introduction to SPH. *Computer Physics Communications*, **48**: 89–96, 1998.
[15] L.B. Lucy. A numerical approach to the testing of the fission hypothesis. *The Astronomical Journal*, **82**: 1013–1024, 1997.
[16] M.S. Khader and M.C. Hanna. An iterarive boundary integral numerical solution for general heat conduction problems, *Journal of Heat Transfer*, **103**: 26–32, 1981.
[17] M.N. Ozisik. *Heat Conduction*, John Wiley & Sons, Singapore 1993.
[18] N. Sukumar, B. Moran and T. Belytschko. The natural element method in solid mechanics, *International Journal for Numerical Methods in Engineering*, **43**: 839–887, 1998.
[19] N. Sukumar, B. Moran, A. Yu Semenov and V.V. Belikov. Natural neighbour Galerkin methods. *International Journal for Numerical Methods in Engineering*, **50**: 1–27, 2001.
[20] R.D. Cook, D.S. Malkus and M.E. Plasha. *Concepts and Applications of Finte Element Analysis*. John Wiley & Sons, Singapore 1989.
[21] S.K. Fraley, T.J. Hoffman and P.N. Stevens. A Monte Carlo method of solving heat conduction problems. *Journal of Heat Transfer*, **102**: 121–125, 1980.
[22] S.N. Atluri, and T. Zhu. A new meshless local Petrov–Galerkin (MLPG) approach in computational mechanics. *Computational Mechanics*, **22**: 117–127, 1998.
[23] S. De and K.J. Bathe. The method of finite spheres. *Computational Mechanics*, **25**: 329–345, 2000.
[24] T. Belytschko, Y.Y. Lu and L. Gu. Element free Galerkin methods. *International Journal of Numerical Methods in Engineering*, **37**: 229–256, 1994.
[25] T. Belytschko, D. Organ and Y. Krongauz. A coupled finite element-element-free Galerkin method. *Computational Mechanics*, **17**: 186–195, 1995.
[26] T. Belytschko, Y. Krongauz, D. Organ, M. Fleming and P. Krysl. Meshless methods: An overview and recent developments. *Computer Methods in Applied Mechanics and Engineering*, **139**: 3–47,1996.
[27] T. Zhu, J.D. Zhang and S.N. Atluri. A meshless local boundary integral equation (LBIE) method for solving nonlinear problems. *Computational Mechanics*, **22**: 174–186, 1998.
[28] W.K. Liu, S. Jun and Y.F. Zhang. Reproducing kernel particle methods. *International Journal for Numerical Methods in Engineering*, **20**: 1081–1106, 1995.
[29] Y.Y. Lu, T. Belytschko, and L. Gu. A new implementation of element free Galerkin method. *Computer Methods in Applied Mechanics and Engineering*, **113**: 397–414, 1994.